Wnt3a links left-right determination with segmentation and anteroposterior axis elongation

Masa-aki Nakaya[1], Kristin Biris[1], Tadasuke Tsukiyama[1], Shaulan Jaime[2], J. Alan Rawls[2] and Terry P. Yamaguchi[1,*]

[1]Cancer and Developmental Biology Laboratory, Center for Cancer Research, National Cancer Institute-Frederick, NIH Frederick, MD 21702, USA
[2]School of Life Sciences, Arizona State University, Tempe, AZ 85287-4501, USA
*Author for correspondence (e-mail: tyamaguchi@ncifcrf.gov)

Accepted 23 September 2005

Development 132, 5425-5436
Published by The Company of Biologists 2005
doi:10.1242/dev.02149

Summary

The alignment of the left-right (LR) body axis relative to the anteroposterior (AP) and dorsoventral (DV) axes is central to the organization of the vertebrate body plan and is controlled by the node/organizer. Somitogenesis plays a key role in embryo morphogenesis as a principal component of AP elongation. How morphogenesis is coupled to axis specification is not well understood. We demonstrate that *Wnt3a* is required for LR asymmetry. *Wnt3a* activates the Delta/Notch pathway to regulate perinodal expression of the left determinant *Nodal*, while simultaneously controlling the segmentation clock and the molecular oscillations of the Wnt/β-catenin and Notch pathways. We provide evidence that Wnt3a, expressed in the primitive streak and dorsal posterior node, acts as a long-range signaling molecule, directly regulating target gene expression throughout the node and presomitic mesoderm. *Wnt3a* may also modulate the symmetry-breaking activity of mechanosensory cilia in the node. Thus, *Wnt3a* links the segmentation clock and AP axis elongation with key left-determining events, suggesting that *Wnt3a* is an integral component of the trunk organizer.

Key words: Mouse, Wnt3a, Left-right determination

Introduction

The anteroposterior (AP) body axis is the first axis to be established during the formation of the mammalian body plan. The left-right (LR) axis is specified last, and is oriented orthogonally to the pre-existing AP and DV axes. The specification and coordination of all three vertebrate body axes is controlled by a small group of cells known as the Spemann-Mangold organizer (Niehrs, 2004). A transient structure, termed the node, is generally considered to be the murine equivalent of the Spemann-Mangold organizer; however, the node first forms at the anterior end of the primitive streak of the gastrulating embryo on embryonic day (E) 7.5, well after AP polarity has been established. The timing of node formation correlates well with LR axis specification, and with the beginning of somitogenesis and the development of the trunk. Somitogenesis generates the segmental structures of the trunk and is a major morphogenetic force driving the elongation of the AP axis. The node plays an important role in trunk development as node ablation results in the loss of LR and dorsoventral (DV) polarity, retarded somite formation and shortened trunks (Davidson et al., 1999). Thus, the node functions as a trunk organizer, coordinating axis determination with trunk elongation.

Members of the transforming growth factor β (Tgfβ) family, specifically *Nodal*, *Lefty1* and *Lefty2*, are the first genes to be asymmetrically expressed along the LR axis (Hamada et al., 2002). *Nodal* is expressed in the periphery of the node, where it functions as the left-determinant (Brennan et al., 2002; Saijoh et al., 2003). *Nodal* transcription is controlled by the Notch signaling pathway. Activation of Notch receptors by the ligand Delta-like 1 (Dll1), leads to the cleavage and nuclear translocation of the Notch intracellular domain, where it acts as a transcription factor when bound to the DNA-binding protein RBP-J (Rbpsuh – Mouse Genome Informatics) (Schweisguth, 2004). Loss of function mutations in components of the Notch pathway lead to loss of LR asymmetry, and RBP-J-binding sites found within the *Nodal* node-specific enhancer are required for *Nodal* expression in the node (Krebs et al., 2003; Raya et al., 2003). These data demonstrate that *Nodal* is a direct target gene of the Notch signaling pathway; however, the relationship between Notch activity and symmetry-breaking events in the node is not clear.

Cilia emanating from the ventral surface of the node play a crucial role in the breaking of bilateral symmetry (McGrath and Brueckner, 2003). Embryos carrying mutations in genes required for cilia formation or motility display laterality defects (Marszalek et al., 1999; Nonaka et al., 1998, Supp et al., 1999). Motile cilia generate a leftward flow of extra-embryonic fluid at the node, termed nodal flow, that is necessary for the generation of LR asymmetry (Nonaka et al., 1998; Okada et al., 1999). Artificial reversal of nodal flow is sufficient to reorient the LR axis (Nonaka et al., 2002) demonstrating that nodal flow is both necessary and sufficient for LR axis specification. These experiments led to the development of the

morphogen flow model that proposed that nodal flow, generated by node cilia, set up a morphogen concentration gradient that directs asymmetric gene expression at the node (Nonaka et al., 1998; Okada et al., 1999).

A second population of node cilia, known as mechanosensory cilia, have been proposed to participate in LR determination, largely owing to the observation that mutations in the polycystic kidney disease 2 (*Pkd2*) gene cause abnormal LR development (Pennekamp et al., 2002). *Pkd2* encodes polycystin 2 (PC2), a Ca^{2+}-permeable cation channel expressed in node cilia that is necessary for the generation of asymmetric Ca^{2+} flux (McGrath et al., 2003). These results led to the development of the two-cilia model for LR initiation in which a centrally located population of Lrd-containing motile cilia generate nodal flow, while a second population of PC2-expressing nonmotile mechanosensory cilia sense nodal flow on the left side of the node and convert it into an asymmetric Ca^{2+}-dependent signal transduction event (McGrath and Brueckner, 2003; Tabin and Vogan, 2003).

Activation of the Wnt/β-catenin pathway by members of the Wnt family of secreted signaling molecules elevates levels of β-catenin, a transcription co-factor with T cell factor/lymphoid enhancer factor (Tcf/Lef), leading to the activation of target genes (see Wnt homepage, http://www.stanford.edu/~rnusse/wntwindow.html). Although it is well-known that Wnts are important molecular components of the vertebrate organizer (Niehrs, 2004), playing crucial roles in AP patterning (Yamaguchi, 2001), little is known about the potential roles that Wnts may play in LR determination. Gain-of-function experiments in the chick embryo have implicated the Wnt/β-catenin pathway in LR patterning (Rodriguez-Esteban et al., 2001); however, loss-of-function mutations have not demonstrated a requirement for Wnts in this process. Interestingly, of the 19 known Wnt genes, *Wnt3a* is the only one whose expression initiates in the gastrulating mouse embryo at E7.5 (Takada et al., 1994), a stage that correlates with node formation, LR determination and somitogenesis. We hypothesized that *Wnt3a* may be an important component of the trunk organizer, functioning to coordinate LR axis specification with trunk development.

Materials and methods

Whole-mount in situ hybridization

The original cDNA clones described in the literature were used as templates for the generation of cRNA probes. Details are available upon request. Whole-mount in situ hybridization was performed as previously described (Wilkinson and Nieto, 1993). Embryos were photographed on a Leica stereoscope or a Zeiss Axiophot compound microscope. Unless indicated otherwise, at least four mutant embryos were examined with each probe, and all yielded similar results.

Antibodies

The following reagents were obtained commercially: mouse monoclonal anti-β-catenin (BD Transduction Laboratories), anti-acetylated tubulin, clone 6-11B-1 (Sigma), goat polyclonal anti-PC1 (M-20) (Santa Cruz), Rhodamine-Phalloidin, DAPI, anti-mouse IgG(H+L) goat Alexa-Fluor 488, anti-goat IgG(H+L) donkey Alexa-Fluor 488 (Molecular Probes), anti-rabbit IgG(H+L) goat Cy3, and anti-mouse IgG(H+L) goat Cy3 and Cy5 (Amersham). The YCC anti-PC2 antibody directed against amino acids 687-962 of human PC2 has been characterized previously (Cai et al., 1999).

Whole-mount immunofluorescence and confocal microscopy

Mouse embryos were fixed with 2% PFA for 20 minutes at room temperature, washed with PBS and stored in 0.1% sodium azide/PBS at 4°C until use. Embryos were permeabilized with 0.1% Triton X-100 and 100 mM glycine in PBS for 10 minutes at room temperature, blocked with 10% calf serum, 0.1% BSA (Sigma) and 3% normal goat serum (NGS) in TBST (20 mM Tris-HCl, pH 8.0, 150 mM NaCl. 0.05% Tween-20), and then incubated with primary or secondary antibodies diluted in TBST containing 0.1% BSA and 1.5% NGS. All blocking and antibody incubation steps were performed overnight at 4°C followed by multiple TBST washes. For imaging (Zeiss LSM510), embryos were placed in Glass Bottom Culture Dishes (MatTek Corporation) in PBS containing 50% Vectashield mounting medium (Vector Labs), or node regions were dissected and mounted on a slide glass with a spacer in SlowFade Light Antifade Kit (Molecular Probes). Four $Wnt3a^{+/-}$ and four $Wnt3a^{-/-}$ 0- to 2-somite stage embryos were analyzed for expression of the cilia markers PC1, PC2 and acetylated tubulin. PC-positive cilia were quantitated manually.

Mice

To make the BAT*lac*Z mouse, two oligos (TBS-1, 5′-AAT TCA GAA TCA TCA AAG GAC CT-3′; and TBS-2, 5′-AAT TAG GTC CTT TGA TGA TTC TG-3′) containing a Tcf/Lef binding site sequence flanked by *Eco*RI sites, were annealed and ligated to construct an 8× multimer, and then subcloned into pBluescript to generate a plasmid designated 8× TBS-pBS. A 130 bp *Xenopus Siamois* minimal promoter was amplified by PCR from p01234 (kindly provided by D. Kimelman) using primers xSiamois-1 (5′-CGT GAA TTC TAT TTA TAT TTT TTT CAT-3′) and xSiamois-2 (5′-AGC GGA TCC CTC TGT CTC CCA AAA TG-3′), and then subcloned into the *Eco*RI/*Bam*HI sites of 8× TBS-pBS. NLS-*lac*Z from pCS-nβ-gal was subcloned into the *Bam*HI/*Xba*I sites of 8× TBS-xSiamois-pBS to generate the BAT*lac*Z transgene. Transgenic mice were generated in the Transgenic Core Facility by pronuclear injection following standard procedures. From the four lines that were generated, the one that most faithfully replicated domains of Wnt signaling was designated as the BAT*LacZ* line. These mice are similar in design to the BATgal mice of Maretto et al. (Maretto et al., 2003). All animal experiments were performed in accordance with the guidelines established by the NCI-Frederick Animal Care and Use Committee.

Results

Wnt3a is expressed in the node and is required for LR axis formation

As a first step towards examining a potential role for *Wnt3a* in LR determination, we directly compared the expression of *Wnt3a* with that of the left determinant *Nodal* by whole-mount in situ hybridization. *Wnt3a* was symmetrically expressed in the primitive streak and dorsal posterior node, immediately adjacent to *Nodal* in the ventral node, during all LR determination stages (E7.75-8.5) (see Fig. S1 in the supplementary material). After the node disappeared (~E8.5), *Wnt3a* remained on in the streak, and later in the tailbud, during all somitogenesis and axis extension stages (Takada et al., 1994).

Examination of E8.75-9.5 embryos homozygous for a null allele of *Wnt3a* (Takada et al., 1994) revealed multiple laterality defects. Although wild-type and $Wnt3a^{+/-}$ hearts invariably looped to the right (Fig. 1A), $Wnt3a^{-/-}$ embryos displayed hearts that looped to the right (45%, n=49) (Fig. 1B), left (31%) (Fig. 1C) or remained in the midline (25%, see Fig.

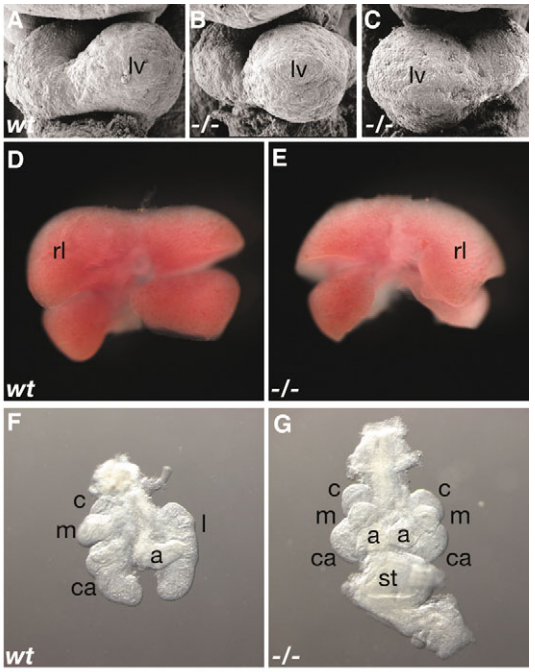

Fig. 1. Loss of *Wnt3a* leads to laterality defects. (A-C) SEM micrographs of E9.5 wild-type (A) and *Wnt3a*$^{-/-}$ (B,C) hearts; mutants displayed normal (B) and inverted (situs inversus) looping (C). (D,E) E11.5 livers. Situs inversus was observed in the asymmetric arrangement of the *Wnt3a*$^{-/-}$ liver (E), compared with the control (D). (F,G) E11.5 lungs and stomach. A midline stomach and right pulmonary isomerism was often observed in mutants (G), in contrast to the wild-type lungs (F, stomach not shown). lv, left ventricle; rl, right lateral lobe; c, cranial lobe; m, medial lobe; ca, caudal lobe; a, accessory lobe; l, left lobe; st, stomach.

S2B in the supplementary material). The direction of axial rotation or embryonic turning was randomized with 47% (n=17) of *Wnt3a*$^{-/-}$ embryos correctly turning clockwise such that the tail and allantois lay on the right side of the embryo, and 53% turning in the opposite direction (not shown). The heart-looping defects were not secondary to earlier defects in cardiogenesis, as several heart markers were expressed normally in the mutants (see Fig. S2 and Fig. S3G-J in the supplementary material).

To assess laterality defects in later-developing visceral organs, we analyzed *Wnt3a*$^{-/-}$ embryos at E11.5-12.5. We were unable to examine the full spectrum of laterality defects as mutants lack posterior organs and generally die by E12.5 (Takada et al., 1994). Nevertheless, we were able to assess the laterality of the heart, lungs, liver and stomach. Of the 19 *Wnt3a*$^{-/-}$ embryos in which multiple organs were assessed, 16 displayed heterotaxy, while the remaining three embryos displayed normal situs. Cardiac laterality was assessed in an additional 20 mutants. Dextrocardia (situs inversus) or abnormal midline positioning of the heart was observed in 38.4% of mutants (n=39). Right pulmonary isomerism, i.e. four lobes on the left and right instead of the single left lobe normally observed in wild-type embryos, was observed 31.6% of the time (n=19; Fig. 1G), while situs ambiguus (two to four lobes on either side) was observed in an additional 21.1%. Left isomerism was not observed. The liver was particularly sensitive to perturbations in left-right determination as 78.9% (n=19) of mutant embryos displayed abnormalities including situs inversus (10.5%) (Fig. 1E) and situs ambiguus (68.4%). Abnormal midline (Fig. 1G), or right-sided, positioning of the stomach was noted 37.5% of the time (n=16). Thus, laterality defects were observed in all of the organs that we were able to assess, indicating that *Wnt3a* plays an early and crucial role in LR determination.

Wnt3a is necessary for asymmetric gene expression

Wnt3a$^{-/-}$ embryos were examined for the expression of the asymmetrically expressed genes *Nodal*, *Lefty1*, *Lefty2* and *Pitx2* at stages prior to the morphological manifestation of LR or AP phenotypes. *Nodal* transcripts were detected in the ventral node of *Wnt3a*$^{-/-}$ mutants at presomitic, headfold (E7.75-8) stages; however, the spatial domain was smaller (Fig. 2B,F) compared with wild-type controls (Fig. 2A,E) (Lowe et al., 1996; Collignon et al., 1996). This domain became increasingly restricted to the posterior edge of the mutant node as development proceeded, and was approximately one-third the size of the wild-type domain (compare Fig. 2H with 2G) by the two- to four-somite stages (Fig. 2D,H,J,N). *Nodal* mRNA was not detected in the *Wnt3a*$^{-/-}$ left lateral plate mesoderm (LPM) at these stages (Fig. 2D) when *Nodal* was normally expressed there in wild-type embryos (Fig. 2C), but was bilaterally expressed in the posterior LPM and streak starting at the four- to five-somite stage (Fig. 2J,N), and remained bilaterally expressed in the LPM (Fig. 2L,P) at stages when *Nodal* was normally turned off in wild-type embryos (six- to eight-somite stages; Fig. 2K,O). The anterior limit of the *Nodal* LPM expression domain was posteriorized in mutants (arrowhead, Fig. 2L), never extending anteriorly into the heart as in earlier staged wild-type embryos (arrowhead, Fig. 2I).

Lefty1 and Lefty2 are required for proper LR patterning, functioning as negative regulators of Nodal (Hamada et al., 2002). *Lefty2* is a direct target gene of Nodal, and is normally expressed in the left LPM between the three- and six-somite stages (Meno et al., 1998) (Fig. 2C,Q,R). *Lefty2* expression in *Wnt3a*$^{-/-}$ embryos mirrored *Nodal* expression, with expression in the LPM initially delayed, then restricted to the posterior streak (Fig. 2D and not shown), and later bilateral and posteriorized (seven somites, Fig. 2Q,R). Similarly, *Pitx2*, a bicoid-type homeobox gene expressed in the left LPM and heart (Yoshioka et al., 1998), was delayed, and then bilaterally expressed in mutant posterior LPM (Fig. 2S; data not shown). *Lefty1* is asymmetrically expressed in the left prospective floor plate (PFP) in wild-type embryos (Meno et al., 1998) (Fig. 2C,G), but was never detected in the mutant PFP, being expressed in only a few individual cells in the posterior node and anterior streak (Fig. 2D,H). Loss of *Lefty1* expression is not due to the physical loss of a midline barrier (Hamada et al., 2002) as several markers, including *Shh*, *Foxa2*, *T*, *Wnt11*, *Gdf1* and cryptic (*Cfc1* – Mouse Genome Informatics) were easily detected in the mutant node, notochord or PFP (see Fig. S3A-L in the supplementary material; data not shown). Thus, molecular marker analyses demonstrate that a cascade of genes necessary for the generation of LR asymmetry are abnormally expressed in the *Wnt3a*$^{-/-}$ node and LPM, indicating that *Wnt3a* functions early in the genetic hierarchy of LR determination.

If *Wnt3a* is upstream of left determining genes, then ectopic

activation of Wnt signaling should alter their expression. To test this, we examined the expression of left determining genes in embryos lacking *Axin*, a negative regulator of the Wnt/β-catenin signaling pathway (Zeng et al., 1997). Homozygous $Axin^{Tg1}$ embryos continued to express *Wnt3a* and *Nodal* normally in the primitive streak; however, *Nodal* expression in the node was slightly expanded (Fig. 2U,W) and large ectopic domains of symmetrical *Nodal* (Fig. 2U) and *Lefty1/2* (Fig. 2W) expression were observed. Thus, both gain- and loss-of-function alleles of genes in the Wnt/β-catenin signaling pathway lead to aberrant expression of left determining genes.

Cilia are structurally normal but display reduced polycystin 1 (PC1) expression

To determine whether a relationship between *Wnt3a* and cilia structure or function exists, we first determined whether cilia were present on the $Wnt3a^{-/-}$ node. Scanning electron microscopy (SEM) analysis of mutant nodes at E7.75 revealed the presence of monocilia in the ventral node (Fig. 3B), similar to that observed in wild-type nodes (Fig. 3A). Immunofluorescent labeling of cilia with anti-acetylated tubulin confirmed this, and further showed that the general morphology of the node remained normal (compare Fig. 3C with 3D; data not shown). Quantitation of node cilia in $Wnt3a^{+/-}$ (mean=158+/–13.7, *n*=4) and $Wnt3a^{-/-}$ (mean=144+/–30.7, *n*=4) stage-matched embryos revealed no significant differences in total cilia number. The presence of structurally normal cilia indicates that Wnt3a does not lie upstream of genes required for ciliary structure, such as *Kif3a* or *Kif3b* as these mutants lack cilia (Marszalek et al., 1999; Nonaka et al., 1998; Takeda et al., 1999).

To assess ciliary motility, we examined $Wnt3a^{-/-}$ embryos for the expression of left-right dynein (*Lrd*; *Dnahc11* – Mouse Genome Informatics), which encodes a ciliary motor protein. *Lrd* was easily detected in the mutant node (Fig. 3E, right embryo). Conversely, *Wnt3a* was normally expressed in inversus viscerum (iv) embryos (which carry a mutation in *Lrd* (Supp et al., 1997)), including embryos that displayed reversed or bilateral *Nodal* expression (Fig. 3F). Crosses between *Wnt3a* and iv did not reveal genetic interactions in transheterozygotes or

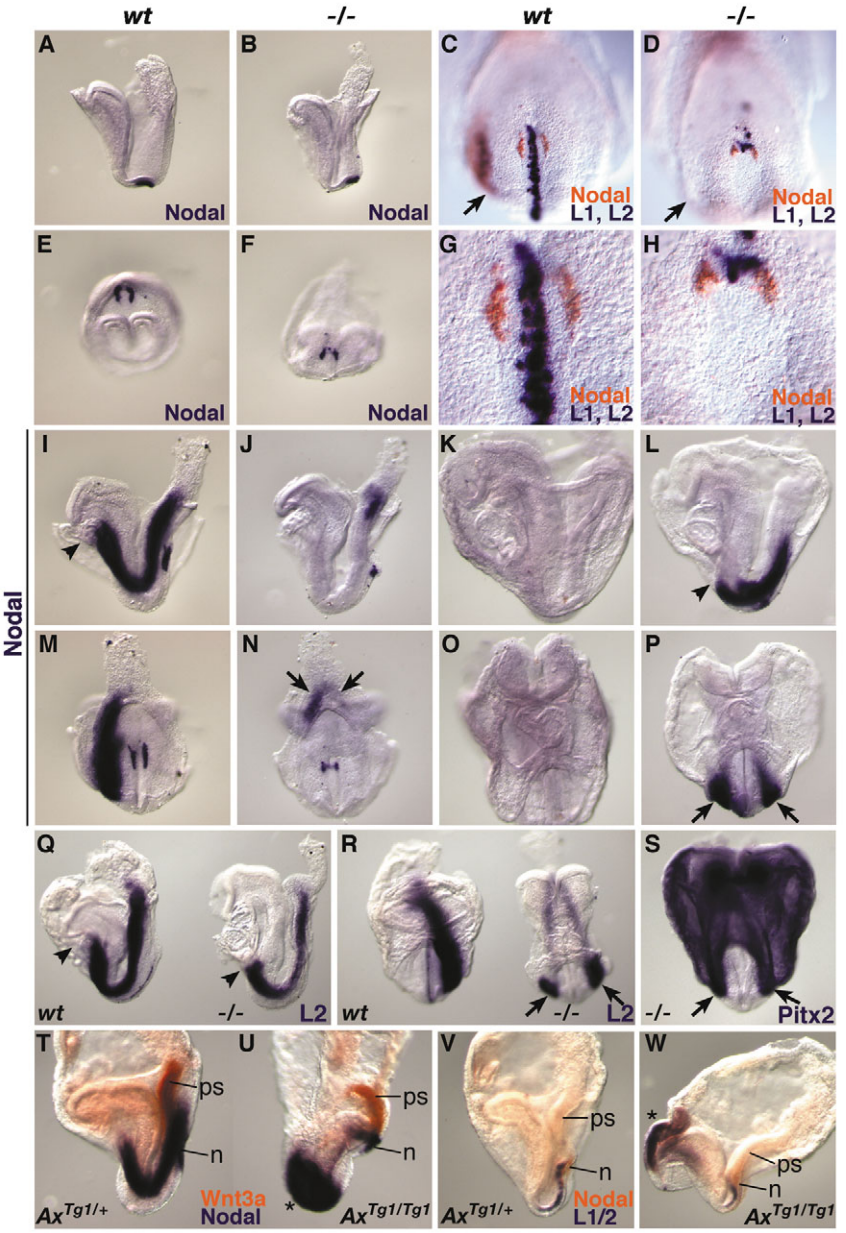

Fig. 2. Wnt signaling controls LR asymmetric gene expression. (A-P) Whole-mount in situ hybridization analysis of *Nodal* expression (see text for details). Headfold-stage wild-type (A,E), and $Wnt3a^{-/-}$ (B,F) embryos express *Nodal* (purple) in the node. Two-color whole-mount in situ hybridization showing *Nodal* (orange), and *Lefty1* and *Lefty2* expression (purple) in wild-type (C,G) and mutant (D,H) three-somite stage embryos. (G,H) High-power ventral views of the nodes of the wild-type and mutant embryos depicted in C,D. *Nodal* expression in wild-type four-somite (I,M) and similarly staged $Wnt3a^{-/-}$ (J,N) embryos. Arrows in N indicate bilateral *Nodal* expression in the mutant posterior LPM. *Nodal* was not expressed in the wild-type LPM after the six- to seven-somite stage (K,O), but was bilaterally expressed in the mutant LPM (L,P). (Q-S) Similar abnormal expression patterns were observed for *Lefty2* in the seven-somite stage mutants (right embryos in Q and R, compare with the four-somite wild-type embryos on the left), and for *Pitx2* expression in six-somite mutants (S). (T,U) Two-color whole-mount in situ hybridization showing *Nodal* (purple) and *Wnt3a* (orange) expression in four-somite wild-type (T) and $Axin^{Tg1/Tg1}$ (U) littermates. (V,W) *Lefty1/2* (purple) and *Nodal* (orange) expression in two-somite wild-type (V) and $Axin^{Tg1/Tg1}$ (W) littermates. Asterisks indicate ectopic bilateral expression of *Nodal* (U) and *Lefty1/2* (W) in anterior domains. (A-D,I-L,Q,T-W) lateral views; (E-H,M,N,S) ventral posterior views; (O,P,R) anterior views; arrows indicate the LPM; arrowheads indicate the anterior limit of LPM expression. ps, primitive streak; n, node.

compound mutants, indicating that *Wnt3a* and iv function in independent genetic pathways (data not shown). In addition, the axonemal dynein heavy chain gene *Dnahc5′* (Ibanez-Tallon et al., 2002) was also expressed in the *Wnt3a*$^{-/-}$ node (not shown). We suggest that ciliary motility was unaffected by the absence of *Wnt3a*.

The presence of mechanosensory cilia in *Wnt3a* mutants was evaluated by examining nodes for the expression of polycystin 1 (PC1) and PC2. The *Pkd1* gene product, PC1, interacts with PC2 and is thought to control the gating of PC2 Ca^{2+} channels (Delmas et al., 2004). While cilia co-expressing PC1, PC2 and acetylated tubulin were easily found in the wild-type node (arrows, Fig. 3J,O), similarly labeled cilia were rarely found in the mutant (Fig. 3N,P,Q). Interestingly, PC1 expression was significantly downregulated (P<0.0001, Welch's t-test) in the *Wnt3a*$^{-/-}$ node cilia (Fig. 3K,N), with only 6.8±5.8% (n=4 embryos) of the mutant cilia expressing detectable levels of PC1, compared with the 46.9±0.9% (n=4) of cilia that were PC1-positive in *Wnt3a*$^{+/-}$ embryos (Fig. 3G,J). PC2 was strongly expressed in more than 92% of central and peripheral cilia in both wild-type and *Wnt3a*$^{-/-}$ nodes (Fig. 3H,L). The rare cilium that co-expressed PC1 and PC2 in *Wnt3a*$^{-/-}$ nodes expressed PC1 weakly and in a much smaller spatial domain (arrow, Fig. 3P) than in wild-type cilia suggesting that mechanotransduction may be perturbed in the absence of *Wnt3a*.

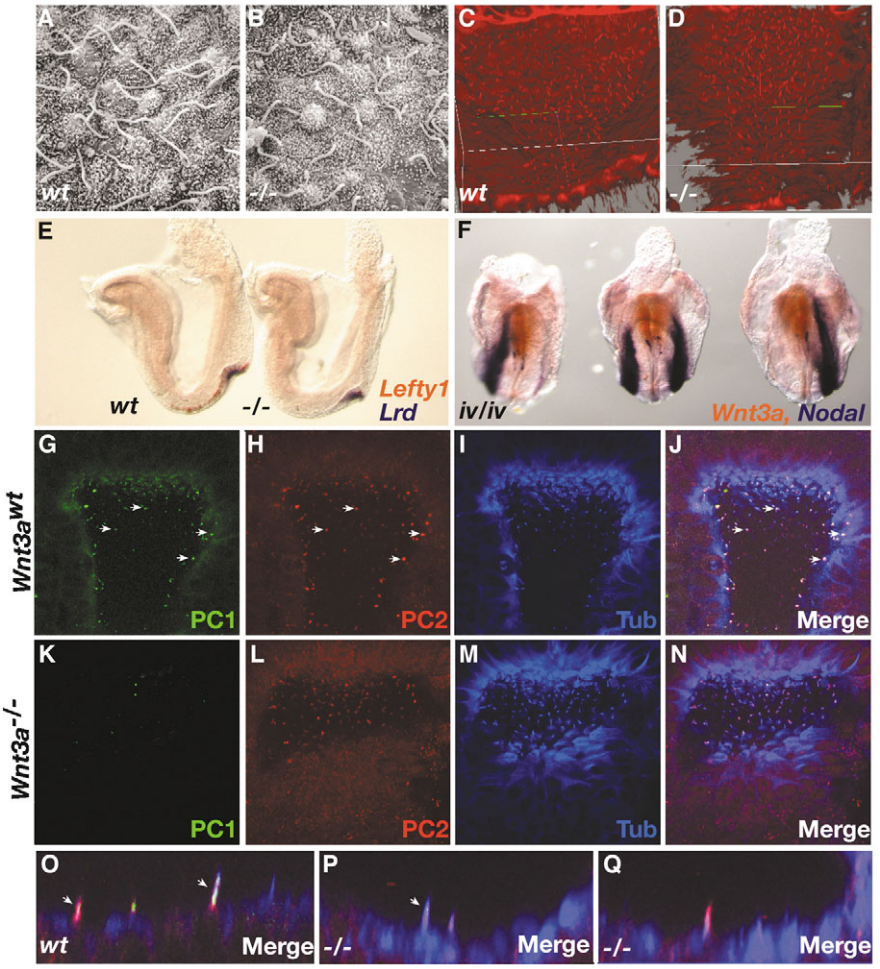

Fig. 3. Examination of cilia in the *Wnt3a*$^{-/-}$ mutants. (A,B) High-power SEM micrographs of cilia in wild-type (A) and *Wnt3a*$^{-/-}$ (B) nodes of head-fold stage embryos (~E7.75-8). (C,D) Projection images of node cilia visualized using anti-acetylated tubulin antibodies. (E) Two-color whole-mount in situ hybridization analysis of *Lefty1* (orange) and *Lrd* (purple) expression in three-somite wild-type (left) and *Wnt3a*$^{-/-}$ (right) embryos. (F) *Wnt3a* (orange) and *Nodal* (purple) expression in three iv/iv embryos. (G-Q) Confocal microscopy images of PC1 (G,K), PC2 (H,L), acetylated tubulin (I,M) and the merged images (J,N,O,P,Q) in E7.75 wild-type (G-J,O) and *Wnt3a*$^{-/-}$ (K-N,P,Q) nodes. The abundance of white spots in global views of the node indicated co-expression of all three markers in individual wild-type cilium (arrows, G-J). By contrast, *Wnt3a*$^{-/-}$ cilia predominantly appeared as purple spots (N), indicating co-expression of only PC2 and tubulin. Views were selected to present sufficient numbers of labeled cilia and therefore depict slightly different regions of the wild-type and mutant node; however, images are representative of the entire node. Profiles of labeled cilia illustrate the co-expression of PC1 and PC2 in distinct spatial domains in wild-type cilia (arrows, O). Rare mutant cilia co-expressed PC1 and PC2 but these domains were unusually small and not easily detected (arrow, P). Cilia co-expressing PC2 and tubulin were easily detected in the mutant node (Q).

Wnt3a signals directly to the node and presomitic mesoderm via β-catenin

Although *Wnt3a* is expressed in the dorsal posterior node, gene expression in the *Wnt3a* mutants is perturbed in both the dorsal and ventral node. To determine which tissues respond directly to Wnt signals, we examined two independent transgenic lines that report sites of presumed Wnt/β-catenin activity in vivo. Both the TOPgal and BAT*lacZ* (see Materials and methods) transgenes were expressed in the node, primitive streak and posterior mesoderm during LR determination stages (Fig. 4A-C,E; see Fig. S4A-C in the supplementary material) (Merrill et al., 2004). The node was the strongest site of β-galactosidase (β-gal) expression in TOPgal embryos at early somite stages (Fig. 4A), with particularly robust expression detected in the ventral node (Fig. 4B).

Although the TOPgal and BAT*lacZ* reporters were both expressed in the node and streak, BAT*lacZ* expression was stronger and extended further anteriorly, through the presomitic mesoderm (psm) where Wnt3a functions to regulate segmentation (Aulehla et al., 2003), to reach an anterior limit at the base of the future hindbrain (compare Fig. 4C with Fig. S4B in the supplementary material). This domain closely paralleled the expression of *Wnt8* (Bouillet et al., 1996). This suggested that the BAT*lacZ* transgene was a more sensitive and accurate reporter of Wnt/β-catenin activity than TOPgal as *Wnt8* and *Wnt3a* are co-expressed at these stages and probably signal via β-catenin. We therefore chose to examine BAT*lacZ*

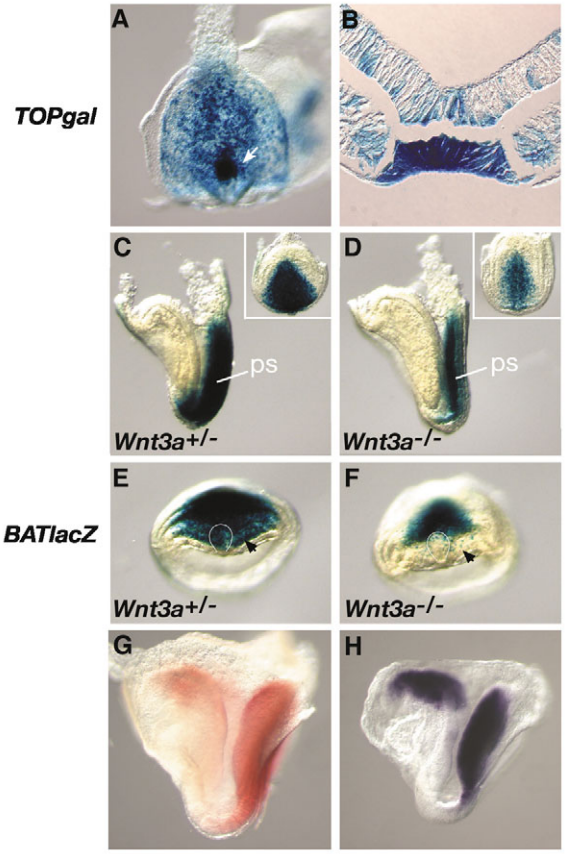

Fig. 4. Expression of Wnt/β-catenin reporter transgenes in vivo is *Wnt3a* dependent. (A) A five-somite TOPgal embryo showed strong expression in the node (arrow), primitive streak (ps) and posterior mesoderm. (B) Cross-section through the node of embryo shown in A. (C,E) A head-fold stage BAT*lac*Z embryo showing β-gal expression in the primitive streak (for posterior view, see inset), anterior psm (black arrow) and the node (curved white line). (D,F) BAT*lac*Z expression was reduced in the *Wnt3a*$^{-/-}$ streak, and was not expressed in the node (curved white line) and anterior psm (black arrow). (G) β-Gal activity in six-somite BAT*lac*Z embryo visualized with Salmon-gal (red). (H) *lac*Z mRNA expression in a five-somite BAT*lac*Z embryo visualized by whole-mount in situ hybridization. (A, and insets in C,D) Ventroposterior views. (E,F) Ventral views, left side of the embryo is on the left. (C,D,G,H) Lateral views, anterior is towards the left.

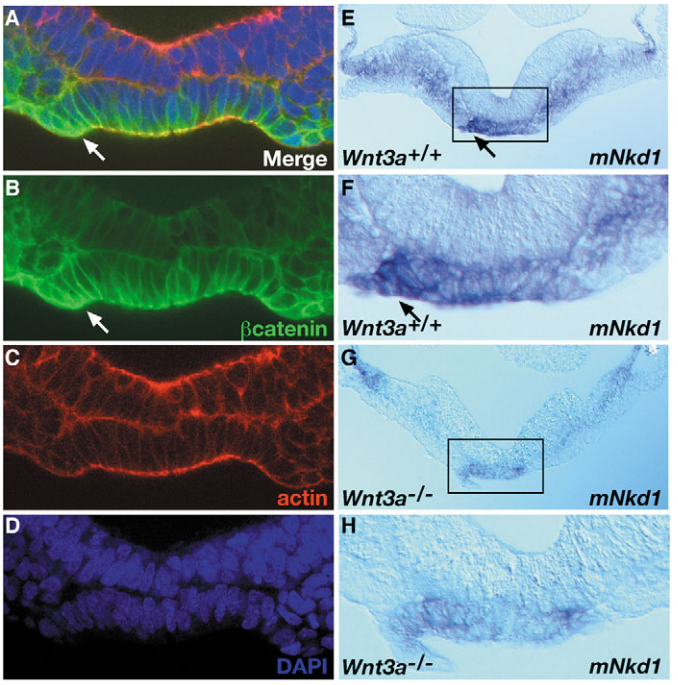

Fig. 5. Asymmetric distribution of canonical Wnt/β-catenin signaling pathway components in the node. All images are posterior views of cross sections, the left side of the embryo is facing left. (A) Merge of confocal microscopy images of E7.75 wild-type embryo labeled with anti-β-catenin antibody (B), rhodamine phalloidin (C) and DAPI (D). (E-H) Expression of the Wnt/β-catenin target gene *Nkd1* in four-somite stage wild-type (E,F) and *Wnt3a*$^{-/-}$ (G,H) embryos. Arrows indicate sites of asymmetric expression in the wild-type node. Boxed regions in E and G are represented as high-power views of the nodes in F and H, respectively. All assessments of *Nkd1* distribution were performed on whole embryos by whole-mount in situ hybridization (not shown), and subsequently sectioned for confirmation and clarity.

expression in the *Wnt3a* mutants. BAT*lacZ* expression was downregulated in the E7.75 primitive streak in the absence of *Wnt3a* (Fig. 4D, inset), compared with controls (Fig. 4C, inset), and was strikingly absent from the node (compare Fig. 4F with Fig. 4E) and anterior psm (arrow, Fig. 4F). This loss of anterior Wnt/β-catenin reporter expression in *Wnt3a*$^{-/-}$ embryos suggests that Wnt3a, emanating from a posterior primitive streak source, functions at a distance to directly activate target genes in the node and anterior psm.

Alternatively, the lack of reporter expression in the mutant node and anterior psm could simply be due to downregulation of the reporter and the consequent reduced levels of the stable β-gal protein. To distinguish between these possibilities, we compared the spatial domain of β-gal activity in BAT*lac*Z embryos with that of the *lac*Z mRNA itself. Whole-mount in situ hybridization revealed that *lac*Z mRNA expression (Fig. 4H) was coincident with β-gal activity (Fig. 4G) and extends into the anterior psm, indicating that the β-gal expression domain is not defined by β-gal stability but rather by direct transcriptional activation of the transgene by Wnt/β-catenin signaling. We suggest that Wnt3a is a long-range signaling molecule capable of activating Wnt/β-catenin target genes in node and anterior psm cells at least 15-20 cell diameters away.

The observation that the Wnt/β-catenin reporters were expressed in the node in a *Wnt3a*-dependent manner strongly indicates that Wnt3a signals in the node via β-catenin. To examine this hypothesis directly, we analyzed the expression of β-catenin in the node during LR axis specification. A transient, subtle, asymmetric gradient of cytoplasmic and membrane-associated β-catenin protein was observed in the node in 50% (8/16) of the E7.75 embryos examined (Fig. 5A,B), with elevated levels found on the left side. Asymmetric β-catenin was not observed in *Wnt3a*$^{-/-}$ embryos at these stages (not shown).

We reasoned that if the transcriptional activator β-catenin was asymmetrically expressed in the node, then target genes of the canonical pathway should also be asymmetrically activated in the node. One such target gene, *Nkd1*, a mammalian

homolog of the Drosophila segment polarity gene *naked cuticle* (Wharton et al., 2001; Yan et al., 2001), was expressed symmetrically in the primitive streak, psm and node at E7.75, but was asymmetrically distributed in the node by the two-somite stage. Elevated levels were observed on the left side of the ventral node, while expression in the psm remained symmetric (Fig. 5E,F). Analysis of *Nkd1* expression in three- to six-somite stage *Wnt3a*$^{-/-}$ embryos (n=4) revealed that transcript levels and asymmetric expression were reduced in the node (Fig. 5G,H). Expression in the mutant psm was also downregulated. Thus, Wnt3a signals directly to the psm and ventral node to activate expression of the Wnt/β-catenin target gene *Nkd1*.

Wnt3a regulates the Dll1/Notch pathway during LR determination and somitogenesis

As the Dll1/Notch signaling pathway directly controls *Nodal* expression in the node (Raya et al., 2003; Krebs et al., 2003), we investigated the possibility that the abnormal *Nodal* expression domain in the *Wnt3a* mutant node may be due to aberrant Notch signaling. Using *Dll1* and *Lfng* as reporters of Notch activity (Raya et al., 2003), we examined Notch activity in *Wnt3a*$^{-/-}$ embryos. At E8, *Dll1* was expressed in the streak and in psm (Fig. 6A) in a pattern similar to the Wnt reporter (Fig. 4C). *Dll1* was expressed in psm cells immediately adjacent to *Nodal*-expressing peripheral ventral node cells (Fig. 6C). Notably, expression of *Dll1* in *Wnt3a*$^{-/-}$ psm was posteriorized such that *Dll1*-expressing cells only contacted the posterior-most node (Fig. 6B,D). This domain correlated well with the abnormally small domain of *Nodal* expression, suggesting that Wnt3a regulates *Nodal* expression indirectly, via Dll1 and the Notch signaling pathway.

To examine whether *Dll1* might function in the same genetic pathway as *Wnt3a*, we crossed *vestigial tail* (*vt*) mice, carrying a hypomorphic allele of *Wnt3a* (Greco et al., 1996), with mice carrying a targeted allele of *Dll1* (Hrabe de Angelis et al., 1997). Analysis of the progeny of *Wnt3a*$^{vt/+}$; *Dll1*$^{+/-}$ animals crossed to *Wnt3a*$^{vt/vt}$ indicated that animals of the expected genotypes were born at Mendelian frequencies but reduced viability of *Wnt3a*$^{vt/+}$; *Dll1*$^{+/-}$ and *Wnt3a*$^{vt/vt}$; *Dll1*$^{+/-}$ compound mutants was observed by weaning stages (see Table S1 in the supplementary material). Examination of offspring at postnatal stages revealed that cardiac abnormalities were the likely cause of the reduced viability. On examination of the hearts, 14.8% of *Wnt3a*$^{vt/+}$; *Dll1*$^{+/-}$ neonatal hearts (n=27; Table 1) displayed situs ambiguus or atrial or ventricular septation defects, and 41.7% of *Wnt3a*$^{vt/vt}$; *Dll1*$^{+/-}$ hearts displayed persistent truncus arteriosis (PTA) (Fig. 6F), transposition of the great arteries (TGA) (Fig. 6G), ventricular

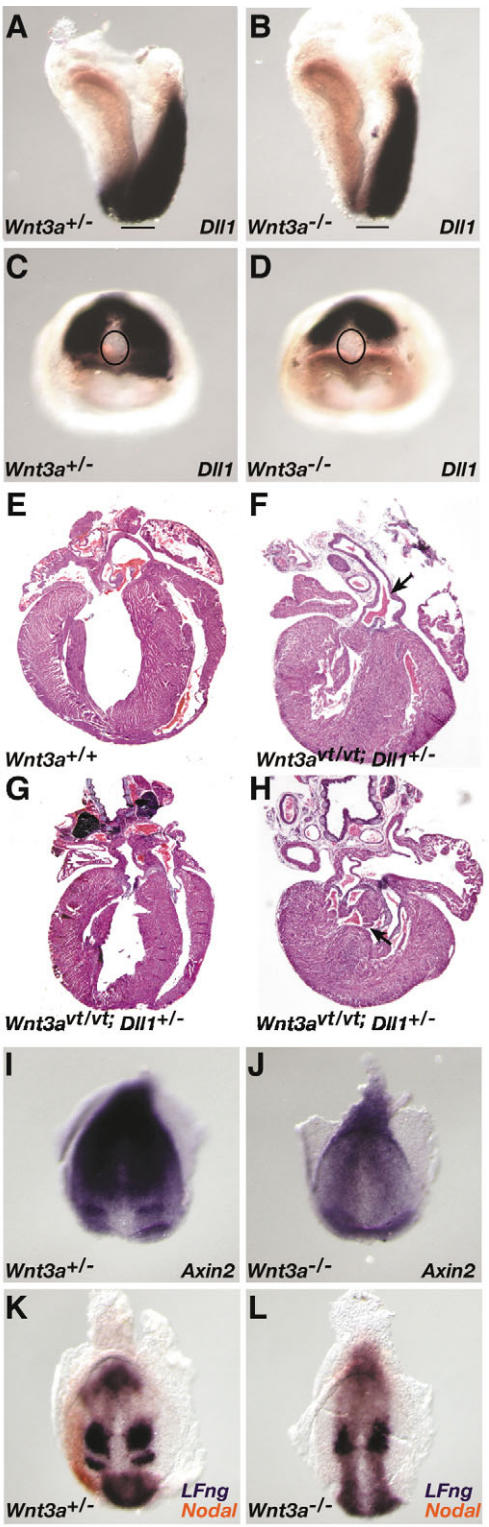

Fig. 6. Components of the Notch pathway participate in a Wnt3a-dependent pathway that controls laterality and somitogenesis. (A-D) Whole-mount in situ hybridization analysis of *Dll1* expression in E8 wild-type (A,C) and *Wnt3a*$^{-/-}$ (B,D) embryos. *Dll1* expression in the psm surrounds the wild-type node (C), but only abuts the posteriormost node in a *Wnt3a*$^{-/-}$ embryo (D). The lines in A and B, and ovals in C and D, indicate the location of the node. (E-H) Histological sections of wild-type neonatal heart (E), and three examples of cardiac laterality defects in compound *Wnt3a*^{vt}; *Dll1* mutants, including PTA (arrow, F), TGA (G) and VSD (arrow, H). (I,J) *Axin2* expression in the streak, psm and in an anterior stripe (presomite 0) in wild-type one-somite embryos (I), was down-regulated in *Wnt3a*$^{-/-}$ mutants and no psm stripes were observed (J). (K,L) Two color whole-mount in situ hybridization on four-somite stage embryos, illustrating (K) cycling *Lfng* (purple) and *Nodal* expression (orange) in the wild-type left LPM. Dynamic *Lfng* expression was not observed in the absence of *Wnt3a*, as only a single psm stripe was observed in the *Wnt3a* mutants (L). Nodal was not expressed in the mutant LPM at these stages.

Table 1. Laterality defects in neonatal offspring from *Wnt3a*$^{vt/+}$/*Dll1*$^{+/-}$ × *Wnt3a*$^{vt/vt}$/*Dll1*$^{+/+}$ cross

Phenotypic trait	*Wnt3a*$^{vt/+}$/*Dll1*$^{+/-}$ (*n*=27)	*Wnt3a*$^{vt/+}$/*Dll1*$^{+/+}$ (*n*=24)	*Wnt3a*$^{vt/vt}$/*Dll1*$^{+/-}$ (*n*=24)	*Wnt3a*$^{vt/vt}$/*Dll1*$^{+/+}$ (*n*=26)
Situs solitis	85.2%	100%	58.3%	100%
Situs inversus or situs ambiguus	3.7%	0%	0%	0%
Atrial or ventricular septa defects	11.1%	0%	29.1%	0%
Transposition of the great arteries	0%	0%	4.2%	
Common truncus arteriosis	0%	0%	4.2%	0%
Stenosis of pulmonary artery	0%	0%	4.2%	0%

septation defects (VSD) (Fig. 6H) or other abnormalities consistent with cardiac laterality defects (Maclean and Dunwoodie, 2004). No other visceral laterality defects were observed. These results suggest that *Wnt3a* and *Dll1* participate in a common genetic pathway to regulate cardiac laterality.

Analysis of the *Wnt3a*^{vt} allele has shown that Wnt3a and the Dll1/Notch pathways play important roles in somitogenesis at tailbud stages (E9.5 onwards), functioning as integral components of the segmentation clock (Aulehla and Herrmann, 2004; Dubrulle and Pourquie, 2004). The temporal and spatial proximity of LR determination (at E7.75-8 in the node), the onset of somitogenesis (at E8 in the adjacent psm), and the common Wnt3a/Dll1 molecular components suggests an intimate relationship between LR determination and somitogenesis. This relationship is strengthened by our demonstration that *Wnt3a* is required for activation of a Wnt/β-catenin reporter in both the node and psm (Fig. 4F). To explore this further, we examined the expression of segmentation clock genes in *Wnt3a*$^{-/-}$ mutants at these earlier stages. *Axin2* is a direct Wnt/β-catenin target gene and negative regulator of the Wnt pathway (Jho et al., 2002; Lustig et al., 2002). It is expressed at E9.5 in a graded oscillating manner in the tailbud and in a single stripe in the anterior psm (Aulehla et al., 2003). At E7.75, *Axin2* is expressed symmetrically in the wild-type node, streak and posterior mesoderm (not shown), and an additional stripe of expression in the anterior psm becomes detectable at early somite stages (Fig. 6I). *Axin2* expression is downregulated in stage-matched *Wnt3a*$^{-/-}$ embryos, and the stripe is no longer detectable in the mutant anterior psm (Fig. 6J).

Lunatic fringe (*Lfng*) expression oscillates in the psm and is dependent upon Notch signaling (Barrantes et al., 1999) and *Wnt3a* (Aulehla et al., 2003) at tailbud stages. At early somitogenesis and LR determination stages when Nodal is expressed in the left LPM, *Lfng* is expressed in a dynamic manner that can manifest in a diffuse patch in the posterior primitive streak and as two stripes adjacent, and anterior, to the node in the psm (Fig. 6K). Interestingly, *Lfng* is also expressed in the node periphery, overlapping with *Nodal* expression in the node (Fig. 6K and not shown). *Wnt3a*$^{-/-}$ mutants (0-7 somites, *n*=7) displayed only a single abnormally shaped stripe of *Lfng* expression posterior to the node and no expression was detected in the node periphery (Fig. 6L). More than one set of stripes was never observed, suggesting that dynamic oscillating *Lfng* expression did not occur in the absence of *Wnt3a*. Together, the *Axin2* and *Lfng* expression patterns indicate that the segmentation clock does not function properly at early somitogenesis stages in the absence of *Wnt3a*. Wnt3a appears to play dual roles at these stages, signaling to the node and psm to regulate LR determination and somitogenesis.

Discussion

We have identified *Wnt3a* as an important new component of the molecular LR determination pathway. *Wnt3a* plays an early role in this process by regulating the expression of the Wnt target gene *Dll1* in the psm, which in turn activates the expression of the left determinant *Nodal* at the psm/node boundary, and regulates somitogenesis in the psm itself (Hrabe de Angelis et al., 1997). Despite the fact that *Wnt3a* transcription is limited to the primitive streak and posterior node, we demonstrate that Wnt3a protein can signal over long distances to directly stimulate gene expression in the node and anterior psm. We confirm and extend the findings of Aulehla et al. (Aulehla et al., 2003) by showing that *Wnt3a* is required for the oscillating expression of the Wnt target gene *Axin2*, as well as the Notch target *Lfng*, in the psm at the onset of somitogenesis. We have also presented evidence that Wnt3a may regulate the function of mechanosensory cilia in the node. Thus, Wnt3a regulates multiple target genes to simultaneously control LR determination and segmentation.

Wnt signaling and organ laterality

Although posterior organs did not develop in *Wnt3a* mutants because of a requirement for *Wnt3a* for posterior development (Takada et al., 1994), laterality phenotypes in anterior viscera such as the heart, lungs and liver were assessed. The majority of E11.5-12.5 *Wnt3a*$^{-/-}$ embryos were heterotaxic, i.e. at least one organ displayed laterality defects. The laterality phenotypes were not secondary to the posterior truncation phenotype as aberrant gene expression in the node was observed well before AP phenotypes emerged. In fact, *Dll1* and *Nodal* are two of the earliest known genes to be affected by the *Wnt3a* mutation and display aberrant expression prior to somitogenesis, arguing that *Wnt3a*, signaling via its target gene *Dll1*, regulates LR determination first, and somitogenesis and AP elongation second.

The process of cardiac looping determines the relative positions of the heart chambers and their connections with the aorta and pulmonary artery. Alterations in the direction of cardiac looping lead to alignment defects that result in a range of cardiovascular abnormalities such as TGA, PTA, double outlet right ventricle (DORV) and atrioventricular septal defects (AVSD) (Maclean and Dunwoodie, 2004). Several of these anomalies were observed in the *Wnt3a*^{vt}*;Dll1* compound mutants, consistent with *Wnt3a* and *Dll1* functioning in a common genetic pathway to regulate cardiac laterality.

The aberrant expression of *Nodal* in *Wnt3a*$^{-/-}$ embryos presents an opportunity to examine the importance of the timing and asymmetric nature of *Nodal* and *Lefty* signaling for organ laterality. As *Nodal* is required in the node to activate *Lefty1* expression in the dorsal node and *Nodal* expression in the LPM (Brennan et al., 2002), we suggest that the reduced

levels of Nodal in the *Wnt3a*$^{-/-}$ node are insufficient to activate *Lefty1* or *Nodal* at the two-somite stage when they are normally activated, but are sufficient to account for the delayed *Nodal* expression observed in the LPM. *Lefty1* was never detected in the mutant PFP, indicating that the midline barrier to Nodal diffusion was absent, and providing an explanation for the bilateral expression of *Nodal* in the >4-somite stage LPM. Interestingly, left pulmonary isomerism was not observed in *Wnt3a* mutants, as would be predicted from the *Lefty1*$^{-/-}$ phenotype (Meno et al., 1998). Instead, the *Wnt3a* mutants more closely resembled cryptic mutants, which lack *Nodal* expression in the LPM and display randomized situs and right isomerism (Yan et al., 1999). As *Nodal* is not expressed bilaterally in the *Wnt3a*$^{-/-}$ LPM until the five-somite stage, these phenotypes suggest that asymmetric *Nodal* expression in the LPM must be established between the two- to four-somite stages (a 6-hour window) to establish proper LR asymmetry in anterior organs. Bilateral *Nodal* expression in the LPM after the five-somite stage appears to be insufficient to induce left isomerisms in any of the organs examined; however, it should be noted that *Nodal* expression in the LPM never extended anteriorly into the heart, as it did in wild-type embryos.

Wnts and polycystins in LR determination

The membrane receptor PC1 colocalizes with PC2 in renal mechanosensory cilia where it senses mechanical bending of the primary cilium induced by fluid flow, transducing it into a chemical Ca^{2+} flux by activating PC2 (Nauli et al., 2003). Kidney cells lacking PC1 form cilia but do not display Ca^{2+} influx when stimulated by fluid flow (Nauli et al., 2003) or activating antibodies (Delmas et al., 2004). Our observation that PC1 is co-expressed with PC2 in node mechanosensory cilia suggests that a similar regulatory relationship between PC1 and PC2 exists in node cilia. Embryos lacking *Wnt3a* display structurally normal node cilia that robustly express PC2 but display reduced levels of PC1. These results predict that Ca^{2+} asymmetry will be perturbed in the *Wnt3a*$^{-/-}$ node, despite the presence of PC2, and this will be addressed in future experiments. As PC1 and PC2 activity appear to be mutually dependent, and mutations in either *Pkd1* or *Pkd2* result in identical polycystic kidney disease phenotypes (Delmas, 2004), it seems likely that *Pkd1* mutants will also display laterality defects and a loss of Ca^{2+} asymmetry. The cardiovascular defects observed in embryos homozygous for a targeted allele of *Pkd1* (Boulter et al., 2001) are consistent with a role for *Pkd1* in the regulation of cardiac laterality.

Despite reports in the literature that *PKD1* is a direct target gene of Wnt/β-catenin signaling (Rodova et al., 2002), our results suggest otherwise. Examination of 5 kb of the mouse *Pkd1* promoter revealed five consensus Tcf1-binding sites; however, activation of the Wnt/β-catenin pathway did not activate *Pkd1* promoter luciferase reporter constructs in transient transfections in vitro (data not shown). Furthermore, mutational analysis showed that the Tcf sites were not necessary for basal expression. It is unclear how Wnt3a indirectly regulates ciliary PC1 expression; however, it is tempting to speculate that the mechanism involves inversin, another ciliary protein required for proper LR determination (Watanabe et al., 2003) that has recently been shown to bind dishevelled and regulate Wnt signaling (Simons et al., 2005).

Wnt3a signaling and target gene expression in the node

Although much of the LR phenotype observed in *Wnt3a* mutants can be directly attributed to the aberrant expression of *Dll1* in the psm, and consequently of *Nodal* in the node, our data indicate that Wnt3a also directly regulates gene expression in the ventral node. Two independent Wnt/β-catenin reporters, as well as the Wnt/β-catenin target genes *Nkd1*and *Axin2*, were expressed there. Interestingly, *Nkd1* expression was asymmetric in the ventral node. The significance of this asymmetric expression, and the mechanisms underlying it, are presently unclear. Given that *Wnt3a* is symmetrically expressed in the streak and node, one possible mechanism, interpreted in the context of the morphogen flow model, is that the Wnt3a ligand itself becomes asymmetrically distributed at the ventral node surface by cilia-generated nodal flow. This hypothesis would require that Wnt3a, which is expressed by the dorsal epiblast, is able to traverse the ventral node epithelium to reach the apical surface of the node where the cilia are located. This is unlikely to occur as the transverse movement of secreted molecules across an epithelial tissue is blocked by the tight junctions of the polarized epithelium. More importantly, this postulate is not supported by our data demonstrating that neither of the Wnt/β-catenin reporters, nor *Axin2*, were asymmetrically expressed in the node. Perhaps a more likely scenario is one in which *Nkd1* is symmetrically activated in the node by Wnt3a, but *Nkd1* mRNA becomes graded because of asymmetric localization or decay. Although *Nkd1* has also been shown to exhibit oscillatory gene expression in the psm (Ishikawa et al., 2004), its function remains unclear as animals lacking *Nkd1* do not display embryonic phenotypes (Li et al., 2005).

Wnt3a is a major component of the trunk organizer

Embryological studies performed primarily in amphibians, fish and chick have demonstrated that the Spemann-Mangold organizer is a dynamic structure that can be subdivided into head, trunk and tail organizers based on their distinct cell subpopulations and differing inductive capacities (Niehrs, 2004). In the mouse, evidence for the distinction of all three organizers remains relatively scant (Robb and Tam, 2004); however, a strong argument can be made for trunk organizer activity residing in the node: (1) transplantation experiments demonstrate that the node is sufficient to induce patterned ectopic trunks, but not heads (Beddington, 1994; Tam et al., 1997); (2) surgical ablation studies show that the node is necessary for DV and LR asymmetry, and proper segmentation and AP elongation of the prospective trunk, but is not required for AP polarity (Davidson et al., 1999). The timing of node formation, which occurs after AP polarity and head structures have been specified, but before LR determination and trunk development, is also consistent with the node functioning as a trunk organizer.

Our demonstration that *Wnt3a* is expressed in the node and is required for LR determination and segmentation, coupled with previous studies demonstrating that *Wnt3a* is required in a dose-dependent manner for the formation of the entire posterior trunk and tail (Greco et al., 1996; Takada et al., 1994), suggests that Wnt3a is a major component of the trunk organizer. We present a model for how Wnt3a could function in this capacity (Fig. 7). A source of Wnt3a is established at

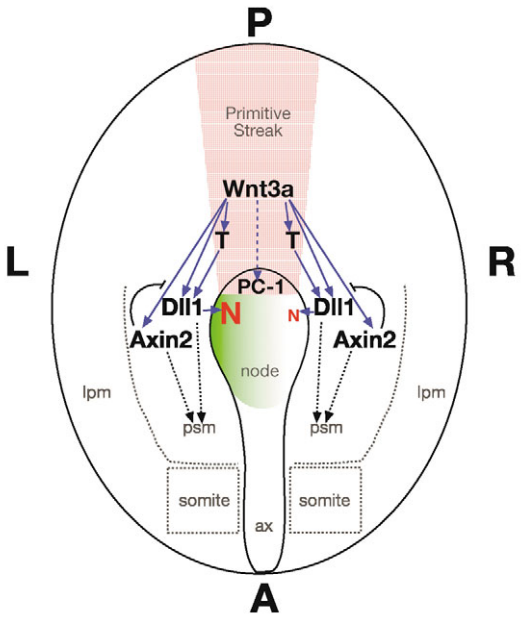

Fig. 7. Wnt3a functions as a trunk organizer. The diagram depicts the ventral view of an E8 embryo. Wnt3a (red stippling) is expressed in the streak and node where it directly activates (solid blue arrows) *T* (brachyury), *Dll1* and *Axin2* via the Wnt/β-catenin pathway. Please see the text for details. Red N, *Nodal*; solid blue arrow, direct gene regulation; broken blue arrow, indirect regulation; green gradient, left-sided Ca^{2+} flux; curved black line, negative feedback loop. Ax, axial mesendoderm.

E7.5 in the primitive streak and node progenitors at the posterior end of the gastrulating embryo. Wnt3a specifies mesoderm fates in the streak by directly regulating *T* transcription (Galceran et al., 2001; Yamaguchi et al., 1999). Wnt3a also regulates *Dll1* expression in the psm directly, and indirectly via T (Galceran et al., 2004; Hofmann et al., 2004). Dll1 expression in the psm stimulates Notch activity at the psm/node boundary, to activate *Nodal* transcription in the node periphery (Krebs et al., 2003; Raya et al., 2003). Activation of *Nodal* in the lateral aspects of the node establishes an axis of *Nodal* expression that is perpendicular to the AP axis, leading to the orthogonal orientation of the LR axis. Elevated Notch activity also activates *Lfng* in the node periphery, which could serve to restrict *Nodal* to the node periphery by inhibiting Notch in a negative-feedback loop (Dale et al., 2003).

The indirect regulation of PC1 expression in the node by Wnt3a may regulate the ability of mechanosensory cilia to interpret symmetry-breaking leftward nodal flow and generate asymmetric Ca^{2+} flux. As alterations in local Ca^{2+} concentrations can affect the affinity of Dll1 for its Notch receptor (Raya et al., 2004), then it is conceivable that Wnt3a could regulate the generation of *Nodal* asymmetry in the node by asymmetrically elevating Ca^{2+} levels on the left side of the node, thereby enhancing Dll1-Notch interactions, and *Nodal* expression, on the left side. Concomitantly, Wnt3a activates *Axin2* in the psm to initiate a Wnt-centered oscillating feedback loop, and Dll1 activates *Lfng* to initiate the Notch-centered oscillating feedback loop (Aulehla and Herrmann, 2004). Together, the two oscillating loops constitute the segmentation clock that controls continued elongation of the trunk and tail along the AP axis. Wnt3a also regulates AP patterning in the trunk and tail by influencing *Cdx1* and *Hox* gene expression (Lohnes, 2003). We propose that Wnt3a functions in the trunk organizer to coordinate patterning and morphogenesis along multiple body axes.

Our work implicates β-catenin as the primary transducer of canonical Wnt signals that coordinately regulate LR specification and segmentation. The use of conditional β-catenin alleles and Cre drivers that are expressed in the node or psm will help address the specific roles that β-catenin plays in the node during LR determination, and in the psm in the regulation of oscillating gene expression during somitogenesis.

We thank D. Epstein, F. Costantini, M. Kuehn, M. Shen, H. Hamada, J. Brennan, D. Kimelman, K. Wharton, M. Brueckner, J. Yost, S. Somlo and A. Gossler for providing reagents and mice. We thank our colleagues at the NCI-Frederick Imaging Facility (S. Lockett and K. Nagashima), and the Transgenic Core Facility (L. Feigenbaum) for their assistance; and C. Stewart, M. Lewandoski, and N. Jenkins for comments on the manuscript. This research was supported by the Intramural Research Program of the NIH, National Cancer Institute, Center for Cancer Research.

Supplementary material

Supplementary material for this article is available at
http://dev.biologists.org/cgi/content/full/132/24/5425/DC1

References

Aulehla, A. and Herrmann, B. G. (2004). Segmentation in vertebrates: clock and gradient finally joined. *Genes Dev.* **18**, 2060-2067.

Aulehla, A., Wehrle, C., Brand-Saberi, B., Kemler, R., Gossler, A., Kanzler, B. and Herrmann, B. G. (2003). Wnt3a plays a major role in the segmentation clock controlling somitogenesis. *Dev. Cell* **4**, 395-406.

Barrantes, I. B., Elia, A. J., Wunsch, K., Hrabe de Angelis, M. H., Mak, T. W., Rossant, J., Conlon, R. A., Gossler, A. and de la Pompa, J. L. (1999). Interaction between Notch signalling and Lunatic fringe during somite boundary formation in the mouse. *Curr Biol.* **9**, 470-480.

Beddington, R. S. (1994). Induction of a second neural axis by the mouse node. *Development* **120**, 613-620.

Bouillet, P., Oulad-Abdelghani, M., Ward, S. J., Bronner, S., Chambon, P. and Dolle, P. (1996). A new mouse member of the Wnt gene family, mWnt-8, is expressed during early embryogenesis and is ectopically induced by retinoic acid. *Mech. Dev.* **58**, 141-152.

Boulter, C., Mulroy, S., Webb, S., Fleming, S., Brindle, K. and Sandford, R. (2001). Cardiovascular, skeletal, and renal defects in mice with a targeted disruption of the Pkd1 gene. *Proc. Natl. Acad. Sci. USA* **98**, 12174-12179.

Brennan, J., Norris, D. P. and Robertson, E. J. (2002). Nodal activity in the node governs left-right asymmetry. *Genes Dev.* **16**, 2339-2344.

Cai, Y., Maeda, Y., Cedzich, A., Torres, V. E., Wu, G., Hayashi, T., Mochizuki, T., Park, J. H., Witzgall, R. and Somlo, S. (1999). Identification and characterization of polycystin-2, the PKD2 gene product. *J. Biol. Chem.* **274**, 28557-28565.

Collignon, J., Varlet, I. and Robertson, E. J. (1996). Relationship between asymmetric nodal expression and the direction of embryonic turning. *Nature* **381**, 155-158.

Dale, J. K., Maroto, M., Dequeant, M. L., Malapert, P., McGrew, M. and Pourquie, O. (2003). Periodic notch inhibition by lunatic fringe underlies the chick segmentation clock. *Nature* **421**, 275-278.

Davidson, B. P., Kinder, S. J., Steiner, K., Schoenwolf, G. C. and Tam, P. P. (1999). Impact of node ablation on the morphogenesis of the body axis and the lateral asymmetry of the mouse embryo during early organogenesis. *Dev. Biol.* **211**, 11-26.

Delmas, P. (2004). Polycystins: from mechanosensation to gene regulation. *Cell* **118**, 145-148.

Delmas, P., Nauli, S. M., Li, X., Coste, B., Osorio, N., Crest, M., Brown, D. A. and Zhou, J. (2004). Gating of the polycystin ion channel signaling complex in neurons and kidney cells. *FASEB J.* **18**, 740-742.

Dubrulle, J. and Pourquie, O. (2004). Coupling segmentation to axis formation. *Development* **131**, 5783-5793.

Galceran, J., Hsu, S. C. and Grosschedl, R. (2001). Rescue of a Wnt mutation by an activated form of LEF-1: regulation of maintenance but not initiation of Brachyury expression. *Proc. Natl. Acad. Sci. USA* **98**, 8668-8673.

Galceran, J., Sustmann, C., Hsu, S. C., Folberth, S. and Grosschedl, R. (2004). LEF1-mediated regulation of Delta-like1 links Wnt and Notch signaling in somitogenesis. *Genes Dev.* **18**, 2718-2723.

Greco, T. L., Takada, S., Newhouse, M. M., McMahon, J. A., McMahon, A. P. and Camper, S. A. (1996). Analysis of the vestigial tail mutation demonstrates that Wnt-3a gene dosage regulates mouse axial development. *Genes Dev.* **10**, 313-324.

Hamada, H., Meno, C., Watanabe, D. and Saijoh, Y. (2002). Establishment of vertebrate left-right asymmetry. *Nat. Rev. Genet.* **3**, 103-113.

Hofmann, M., Schuster-Gossler, K., Watabe-Rudolph, M., Aulehla, A., Herrmann, B. G. and Gossler, A. (2004). WNT signaling, in synergy with T/TBX6, controls Notch signaling by regulating Dll1 expression in the presomitic mesoderm of mouse embryos. *Genes Dev.* **18**, 2712-2717.

Hrabe de Angelis, M., McIntyre, J., 2nd and Gossler, A. (1997). Maintenance of somite borders in mice requires the Delta homologue DII1. *Nature* **386**, 717-721.

Ibanez-Tallon, I., Gorokhova, S. and Heintz, N. (2002). Loss of function of axonemal dynein Mdnah5 causes primary ciliary dyskinesia and hydrocephalus. *Hum. Mol. Genet.* **11**, 715-721.

Ishikawa, A., Kitajima, S., Takahashi, Y., Kokubo, H., Kanno, J., Inoue, T. and Saga, Y. (2004). Mouse Nkd1, a Wnt antagonist, exhibits oscillatory gene expression in the PSM under the control of Notch signaling. *Mech. Dev.* **121**, 1443-1453.

Jho, E. H., Zhang, T., Domon, C., Joo, C. K., Freund, J. N. and Costantini, F. (2002). Wnt/beta-catenin/Tcf signaling induces the transcription of Axin2, a negative regulator of the signaling pathway. *Mol. Cell. Biol.* **22**, 1172-1183.

Kispert, A., Vainio, S. and McMahon, A. P. (1998). Wnt-4 is a mesenchymal signal for epithelial transformation of metanephric mesenchyme in the developing kidney. *Development* **125**, 4225-4234.

Krebs, L. T., Iwai, N., Nonaka, S., Welsh, I. C., Lan, Y., Jiang, R., Saijoh, Y., O'Brien, T. P., Hamada, H. and Gridley, T. (2003). Notch signaling regulates left-right asymmetry determination by inducing Nodal expression. *Genes Dev.* **17**, 1207-1212.

Li, Q., Ishikawa, T., Miyoshi, H., Oshima, M. and Taketo, M. M. (2005). A targeted mutation of Nkd1 impairs mouse spermatogenesis. *J. Biol. Chem.* **280**, 2831-2839.

Lohnes, D. (2003). The Cdx1 homeodomain protein: an integrator of posterior signaling in the mouse. *BioEssays* **25**, 971-980.

Lowe, L. A., Supp, D. M., Sampath, K., Yokoyama, T., Wright, C. V., Potter, S. S., Overbeek, P. and Kuehn, M. R. (1996). Conserved left-right asymmetry of nodal expression and alterations in murine situs inversus. *Nature* **381**, 158-161.

Lustig, B., Jerchow, B., Sachs, M., Weiler, S., Pietsch, T., Karsten, U., van de Wetering, M., Clevers, H., Schlag, P. M., Birchmeier, W. et al. (2002). Negative feedback loop of Wnt signaling through upregulation of conductin/axin2 in colorectal and liver tumors. *Mol. Cell. Biol.* **22**, 1184-1193.

Maclean, K. and Dunwoodie, S. L. (2004). Breaking symmetry: a clinical overview of left-right patterning. *Clin. Genet.* **65**, 441-457.

Maretto, S., Cordenonsi, M., Dupont, S., Braghetta, P., Broccoli, V., Hassan, A. B., Volpin, D., Bressan, G. M. and Piccolo, S. (2003). Mapping Wnt/beta-catenin signaling during mouse development and in colorectal tumors. *Proc. Natl. Acad. Sci. USA* **100**, 3299-3304.

Marszalek, J. R., Ruiz-Lozano, P., Roberts, E., Chien, K. R. and Goldstein, L. S. (1999). Situs inversus and embryonic ciliary morphogenesis defects in mouse mutants lacking the KIF3A subunit of kinesin-II. *Proc. Natl. Acad. Sci. USA* **96**, 5043-5048.

McGrath, J. and Brueckner, M. (2003). Cilia are at the heart of vertebrate left-right asymmetry. *Curr. Opin. Genet. Dev.* **13**, 385-392.

McGrath, J., Somlo, S., Makova, S., Tian, X. and Brueckner, M. (2003). Two populations of node monocilia initiate left-right asymmetry in the mouse. *Cell* **114**, 61-73.

Meno, C., Shimono, A., Saijoh, Y., Yashiro, K., Mochida, K., Ohishi, S., Noji, S., Kondoh, H. and Hamada, H. (1998). lefty-1 is required for left-right determination as a regulator of lefty-2 and nodal. *Cell* **94**, 287-297.

Merrill, B. J., Pasolli, H. A., Polak, L., Rendl, M., Garcia-Garcia, M. J., Anderson, K. V. and Fuchs, E. (2004). Tcf3: a transcriptional regulator of axis induction in the early embryo. *Development* **131**, 263-274.

Nauli, S. M., Alenghat, F. J., Luo, Y., Williams, E., Vassilev, P., Li, X., Elia, A. E., Lu, W., Brown, E. M., Quinn, S. J. et al. (2003). Polycystins 1 and 2 mediate mechanosensation in the primary cilium of kidney cells. *Nat. Genet.* **33**, 129-137.

Niehrs, C. (2004). Regionally specific induction by the Spemann-Mangold organizer. *Nat. Rev. Genet.* **5**, 425-434.

Nonaka, S., Tanaka, Y., Okada, Y., Takeda, S., Harada, A., Kanai, Y., Kido, M. and Hirokawa, N. (1998). Randomization of left-right asymmetry due to loss of nodal cilia generating leftward flow of extraembryonic fluid in mice lacking KIF3B motor protein. *Cell* **95**, 829-837.

Nonaka, S., Shiratori, H., Saijoh, Y. and Hamada, H. (2002). Determination of left-right patterning of the mouse embryo by artificial nodal flow. *Nature* **418**, 96-99.

Okada, Y., Nonaka, S., Tanaka, Y., Saijoh, Y., Hamada, H. and Hirokawa, N. (1999). Abnormal nodal flow precedes situs inversus in iv and inv mice. *Mol. Cell* **4**, 459-468.

Pennekamp, P., Karcher, C., Fischer, A., Schweickert, A., Skryabin, B., Horst, J., Blum, M. and Dworniczak, B. (2002). The ion channel polycystin-2 is required for left-right axis determination in mice. *Curr. Biol.* **12**, 938-943.

Raya, A., Kawakami, Y., Rodriguez-Esteban, C., Buscher, D., Koth, C. M., Itoh, T., Morita, M., Raya, R. M., Dubova, I., Bessa, J. G. et al. (2003). Notch activity induces Nodal expression and mediates the establishment of left-right asymmetry in vertebrate embryos. *Genes Dev.* **17**, 1213-1218.

Raya, A., Kawakami, Y., Rodriguez-Esteban, C., Ibanes, M., Rasskin-Gutman, D., Rodriguez-Leon, J., Buscher, D., Feijo, J. A. and Izpisua Belmonte, J. C. (2004). Notch activity acts as a sensor for extracellular calcium during vertebrate left-right determination. *Nature* **427**, 121-128.

Robb, L. and Tam, P. P. (2004). Gastrula organiser and embryonic patterning in the mouse. *Semin. Cell Dev. Biol.* **15**, 543-554.

Rodova, M., Islam, M. R., Maser, R. L. and Calvet, J. P. (2002). The polycystic kidney disease-1 promoter is a target of the beta-catenin/T-cell factor pathway. *J. Biol. Chem.* **277**, 29577-29583.

Rodriguez-Esteban, C., Capdevila, J., Kawakami, Y. and Izpisua Belmonte, J. C. (2001). Wnt signaling and PKA control Nodal expression and left-right determination in the chick embryo. *Development* **128**, 3189-3195.

Saijoh, Y., Oki, S., Ohishi, S. and Hamada, H. (2003). Left-right patterning of the mouse lateral plate requires nodal produced in the node. *Dev. Biol.* **256**, 160-172.

Schweisguth, F. (2004). Notch signaling activity. *Curr. Biol.* **14**, R129-R138.

Simons, M., Gloy, J., Ganner, A., Bullerkotte, A., Bashkurov, M., Kronig, C., Schermer, B., Benzing, T., Cabello, O. A., Jenny, A. et al. (2005). Inversin, the gene product mutated in nephronophthisis type II, functions as a molecular switch between Wnt signaling pathways. *Nat. Genet.* **37**, 537-543.

Supp, D. M., Brueckner, M., Kuehn, M. R., Witte, D. P., Lowe, L. A., McGrath, J., Corrales, J. and Potter, S. S. (1999). Targeted deletion of the ATP binding domain of left-right dynein confirms its role in specifying development of left-right asymmetries. *Development* **126**, 5495-5504.

Tabin, C. J. and Vogan, K. J. (2003). A two-cilia model for vertebrate left-right axis specification. *Genes Dev.* **17**, 1-6.

Takada, S., Stark, K. L., Shea, M. J., Vassileva, G., McMahon, J. A. and McMahon, A. P. (1994). Wnt-3a regulates somite and tailbud formation in the mouse embryo. *Genes Dev.* **8**, 174-189.

Takeda, S., Yonekawa, Y., Tanaka, Y., Okada, Y., Nonaka, S. and Hirokawa, N. (1999). Left-right asymmetry and kinesin superfamily protein KIF3A: new insights in determination of laterality and mesoderm induction by kif3A–/– mice analysis. *J. Cell Biol.* **145**, 825-836.

Tam, P. P., Steiner, K. A., Zhou, S. X. and Quinlan, G. A. (1997). Lineage and functional analyses of the mouse organizer. *Cold Spring Harb. Symp. Quant. Biol.* **62**, 135-144.

Watanabe, D., Saijoh, Y., Nonaka, S., Sasaki, G., Ikawa, Y., Yokoyama, T. and Hamada, H. (2003). The left-right determinant Inversin is a component of node monocilia and other 9+0 cilia. *Development* **130**, 1725-1734.

Wharton, K. A., Jr, Zimmermann, G., Rousset, R. and Scott, M. P. (2001). Vertebrate proteins related to Drosophila Naked Cuticle bind Dishevelled and antagonize Wnt signaling. *Dev. Biol.* **234**, 93-106.

Wilkinson, D. G. and Nieto, M. A. (1993). Detection of messenger RNA by in situ hybridization to tissue sections and whole mounts. *Methods Enzymol.* **225**, 361-373.

Yamaguchi, T. P. (2001). Heads or tails: Wnts and anterior-posterior patterning. *Curr. Biol.* **11**, R713-R724.

Yamaguchi, T. P., Takada, S., Yoshikawa, Y., Wu, N. and McMahon, A. P.

(1999). T (Brachyury) is a direct target of Wnt3a during paraxial mesoderm specification. *Genes Dev.* **13**, 3185-3190.

Yan, D., Wallingford, J. B., Sun, T. Q., Nelson, A. M., Sakanaka, C., Reinhard, C., Harland, R. M., Fantl, W. J. and Williams, L. T. (2001). Cell autonomous regulation of multiple Dishevelled-dependent pathways by mammalian Nkd. *Proc. Natl. Acad. Sci. USA* **98**, 3802-3807.

Yoshioka, H., Meno, C., Koshiba, K., Sugihara, M., Itoh, H., Ishimaru, Y., Inoue, T., Ohuchi, H., Semina, E. V., Murray, J. C. et al. (1998). Pitx2, a bicoid-type homeobox gene, is involved in a lefty-signaling pathway in determination of left-right asymmetry. *Cell* **94**, 299-305.

Zeng, L., Fagotto, F., Zhang, T., Hsu, W., Vasicek, T. J., Perry, W. L., 3rd, Lee, J. J., Tilghman, S. M., Gumbiner, B. M. and Costantini, F. (1997). The mouse Fused locus encodes Axin, an inhibitor of the Wnt signaling pathway that regulates embryonic axis formation. *Cell* **90**, 181-192.